Colloid Polym Sci (2013) 291:2879–2892
DOI 10.1007/s00396-013-3007-9

ORIGINAL CONTRIBUTION

Solvent induced phenomena in a dendronized linear polymer

Anja Kroeger · Baozhong Zhang · Christine Rosenauer · A. Dieter Schlüter · Gerhard Wegner

Received: 22 April 2013 / Revised: 6 June 2013 / Accepted: 7 June 2013 / Published online: 7 August 2013

Abstract The properties of a dendronized linear polymer (DP) in dilute solutions depending on solvent quality and temperature are described. The polymer has a contour length of L_c=1,060 nm. The sample of the fourth generation (PG4) was analyzed in the thermodynamically good solvents dioxane, chloroform, and methanol. The wormlike macromolecule has a persistence length l_p=7 nm in dioxane and a cross-section radius determined by small angle X-ray scattering (SAXS) of $R_{c\ (SAXS)}$=2.8 nm. The bulk density of PG4 determined by SAXS was compared with solution density. Evidence for substantial swelling of the cross-section was found. Toluene acts as a thermodynamically poor solvent (θ solvent). Above the θ temperature T_θ, a strong temperature dependence of the size and the Young's modulus E was observed. Following Odijk, E/k_BT ~1 was found. Below T_θ, a regime characterized by unswelling of the wormlike chains was observed. The results suggest that DPs can be described as soft colloid filaments, which are subject to commonly observed interactions in colloidal systems. A phase diagram indicates a regime below T_θ in which fluctuations of osmotic pressure inside the filaments result in periodic undulation of the chains. In summary, introducing a dense dendritic shell around the backbone converts conventional polymers into molecular colloids.

Keywords Dendronized polymers · Solution behavior · Phase separation · Colloidal filaments · Morphological instability

Introduction

Ever since dendronized linear polymers (DPs) have come to the scene [1–17], the question was raised whether such structures exhibit properties fundamentally or—at least—substantially different from ordinary linear polymers that are furnished with small but sterically assuming side groups. Poly(*tert*-butyl-methacrylate) (P*t*BMA) is a simple example for such a case in which steric interactions among the side groups enlarge the stiffness of the macromolecule substantially. The latter is inferred from comparison of the characteristic ratio of P*t*BMA and polymethyl methacrylate (PMMA) [18]. It is ~11 for the former, meaning that the respective Kuhn length l_k, which is the length of the statistical element of the random flight chain, amounts to 2.8 nm while it is ~7 for atactic PMMA translating in l_k=1.8 nm [19].

Considering the case in which each repeat unit of the linear backbone is furnished with a dendron of given generation, this question was treated from a theoretical point of view first by Halperin and coworkers [20] and more recently by Borisov et al.[21]. Both groups compare DPs as the one extreme case with bottlebrush-type polymers as the other limiting case of densely substituted linear chains. Both groups used the well-known tools of statistical physics of macromolecules. These studies provide scaling laws which predict the average thickness of the cross section of the respective polymers pending on the parameters: dendron generation and chain length of the linear side groups forming brushes, respectively, as well as periodicity of substitution along the chain. Most recently, an atomistic molecular dynamics (MD) simulation of the same DP as studied experimentally in this work has been published [22]. This computer simulation considers the DPs both under

Electronic supplementary material The online version of this article (doi:10.1007/s00396-013-3007-9) contains supplementary material, which is available to authorized users.

A. Kroeger (✉) · C. Rosenauer · G. Wegner
Max Planck Institute for Polymer Research,
Ackermannweg 10, 55128 Mainz, Germany
e-mail: kroeger@mpip-mainz.mpg.de

B. Zhang · A. D. Schlüter
Laboratory of Polymer Chemistry, Department of Materials,
ETH Zurich, Wolfgang-Pauli-Strasse 10,
HCI J541, 8093 Zurich, Switzerland

solvent-free conditions and equilibrated with chloroform as solvent.

A further theoretical study on the size and shape of DPs in solution and various effects of the solvent quality was performed by Kosmas et al. [23]. Such theoretical work based on statistical molecular mechanics lacks the assessment of the specific solvent–segment interactions for which the interaction of solvent with hydrogen-bonded residues in the branches of the dendrons may serve as an example. Therefore, theoretical treatments as found in the present literature are valuable in that they point to principal differences between dendronized and bottlebrush polymers but they cannot predict the true cross-section diameter nor the persistence length of real polymers dissolved in real solvents.

Moreover, the question may be raised to what extent the intramolecular interactions among the segments and their intermolecular contacts would not be suitably described by elements of the Derjaguin–Landau–Verwey–Overbeek (DLVO) theory [24–26]. As much as the interaction among spherical polymer particles for which either conventional dendrimers or internally cross-linked gel particles serve as examples are governed by the forces described by the DLVO theory [27, 28], a DP could potentially be described as a colloidal filament of very large aspect ratio.

The synthesis of DPs is well established [1–17, 29] and important details concerning the structural purity that is the nature and perfection of the branches in each generation have been laid open [30]. Determination of the molecular weight by light scattering has been successfully demonstrated for the case of a thermodynamically good solvent [31]. However, detailed studies of the solution properties depending on solvent quality are lacking so far. Such studies would help to reveal the features in which DPs differ in a principal manner from ordinary linear polymers. An exception is the recent work on water-soluble DPs in which the dendrons comprised water-compatible segments of oligo(oxyethylene) groups. These DPs when dissolved in water showed a phase separation behavior with a lower critical solution temperature (LCST). Detailed studies making use of ESR labels indicated that the corona of the dendrons exhibits complex dynamics both below and above the LCST [32–34]. This was the first time that a feature was revealed which cannot be observed for conventional linear polymers.

This work describes the solution behavior of a paradigmatic DP with the chemical structure shown in Fig. 1, named PG4, where every repeat unit of the poly(methacrylate) backbone carries one dendron of the fourth generation. The synthetic route and characterization procedure for this polymer has been described in great details [20, 35]. PG4 exhibits a weight average degree of polymerization of P_W=4,240, resulting in a contour length of L_c=1,060 nm. The aspect ratio, defined here, as the ratio of the contour length to the cross-section diameter is A » 100 and the polymer is soluble in a number of quite different organic solvents such as chloroform, dioxane, and methanol.

The investigations described in this paper deal with the following questions: How do cross-section radius, radius of gyration, hydrodynamic radius, and persistence length depend on solvent quality? Is it possible to identify a θ solvent and what is the solution behavior around the theta-temperature T_θ? This also implies the question: what is the meaning of T_θ in the case of DPs? All these questions aim at creating an understanding for what the differences between conventional and dendronized polymers are.

In consequence, this paper is arranged as follows: Solutions of PG4 in different thermodynamically good solvents are studied in the first section. Molecular weights, radii of gyration, and persistence lengths are evaluated by static light scattering experiments (SLS) and hydrodynamic radii are determined by dynamic light scattering (DLS). Moreover, density measurements give insight into the dependence of the cross-section radii on the solvent quality. Finally, the behavior of the DP in a θ solvent above and below T_θ is treated. A model, in which PG4 is considered as a filament of colloidal nature undergoing shape fluctuations depending on solvent quality and temperature, will be presented at the end.

Experimental section

Materials Dendronized poly(methyl acrylate), named PG4, where the last digit refers to the generation number G, was synthesized using a divergent growth protocol based on Merrifield peptide synthesis. The details of the synthesis are described elsewhere [20, 35]. Sample solutions of PG4 of a polymer concentration c=1 g L^{-1} for light scattering experiments were prepared by dissolving PG4 in toluene, dioxane, or chloroform under continuous stirring for 18 h at a temperature T=45 °C (toluene) and at room temperature (dioxane and chloroform). Toluene (p. a.≥99.7 %), 1,4-dioxane (p. a.≥99.5 %), and chloroform (p. a.≥99.8 %) were purchased from Sigma-Aldrich and used without further purification. Freshly prepared solutions were always used.

Photon correlation spectroscopy SLS and DLS experiments were performed on an ALV spectrometer consisting of a goniometer and an ALV-5004 multiple-tau full-digital correlator (320 channels), which allows measurements over a time range $10^{-7} \le t \le 10^{3}$ s and an angular range from 20° to 150° corresponding to a scattering vector $q = 4.8 \cdot 10^{-3}$–$2.6 \cdot 10^{-2}$ nm^{-1}. A He-Ne laser (uniphase with a single mode intensity of 25 mW operating at a laser wavelength of $\lambda_{0\ LS}$=632.8 nm) was used as light source. In this setup, only vertically polarized incident laser light and no polarizer (analyzer) in the scattered light beam pathway is used. For

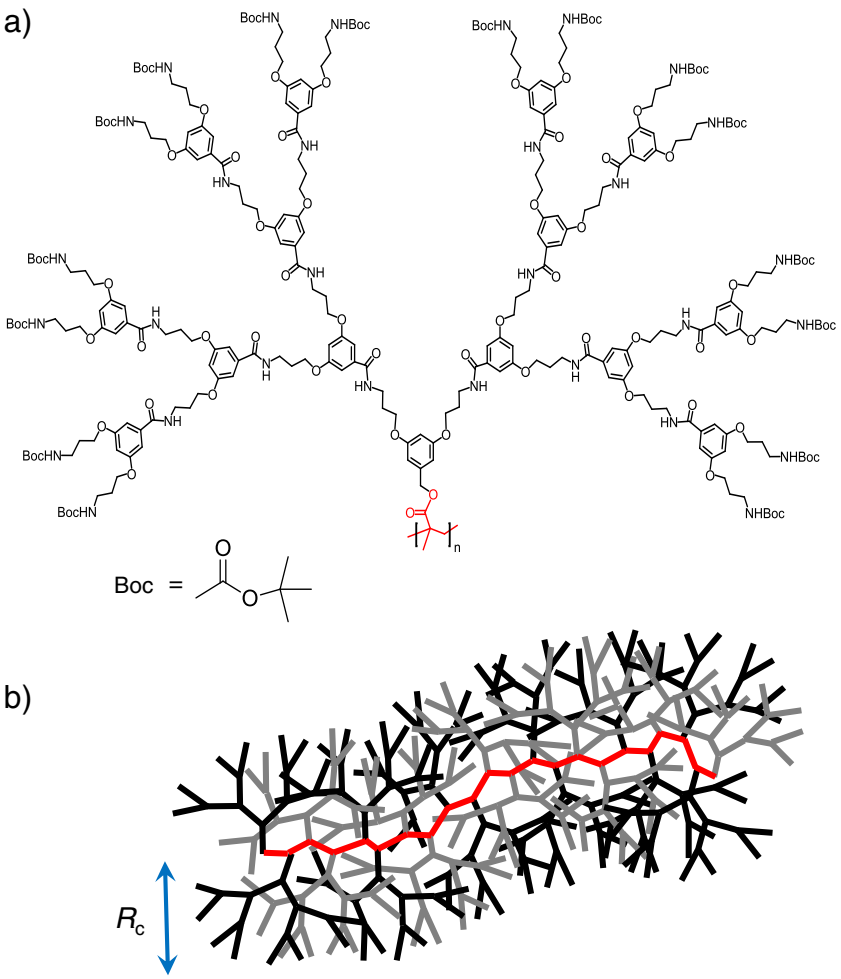

Fig. 1 **a** Chemical structure of a fourth generation DP (PG4), where *n* refers to the number of monomeric units (degree of polymerization) and Boc stands for *tert*-butyloxycarbonyl. **b** Schematic picture of the primary structure of the polymer giving a pictorial view on the entanglement network formed by the dendron branches; R_c indicates the cross-section radius of the macromolecule

temperature-controlled experiments, the light scattering instrument was equipped with a thermostat from Julabo. Dust-free solutions for SLS and DLS experiments were obtained by filtration through PTFE membrane filters with a pore size of 5 μm (Millipore LCR syringe filters) directly into cylindrical silica glass cuvettes (Hellma, inner diameter ∅=10 mm), which had been cleaned before with acetone in a Thurmont apparatus. The theoretical details of the DLS experiments and specifics of the data evaluation by using the stretched exponential Kohlrausch–Williams–Watt (KWW) function are given elsewhere [36, 37]. This method assumes that the computed relaxation function $C(q,t)$ can be represented by

$$C(q,t) = \exp\left[-\left(t\Big/\tau \times (q)\right)^{\beta}\right] \quad (1)$$

where the shape parameter $0<\beta\leq 1$ characterizes the distribution of relaxation times τ.

SLS experiments were performed with the same instrumental setup. The reduced absolute intensity ratio $R(q)/(Kc)$ at a polymer concentration c is computed from the Rayleigh ratio $R(q)$ and the optical constant $K=(2\pi n\, \mathrm{d}n/\mathrm{d}c)^2/(\lambda_{0\,\mathrm{LS}}{}^4 N_A)$; pure toluene is used as a standard with refractive index n_t and Rayleigh ratio $R_t=2.2\cdot 10^{-5}$ cm^{-1} whereas N_A is the Avogadro number [38, 39]. For SLS experiments, samples solved in dioxane, chloroform, and toluene (c=0.25—5 g L^{-1}) were prepared as described above. The refractive index increment $\mathrm{d}n/\mathrm{d}c=0.1469$ mL g^{-1} (for PG4 in dioxane) and $\mathrm{d}n/\mathrm{d}c=0.0948$ mL g^{-1} (for PG4 in chloroform) were measured at room temperature at $\lambda_0=633$ nm using a scanning Michelson interferometer [40].

Small angle X-ray scattering All experiments were performed at a self-built small angle X-ray scattering (SAXS) facility equipped with a X-ray generator with Cu anode, CuK alpha radiation (wavelength $\lambda_{0\,x}=1.54$ Å), Rigaku MicroMax

007, curved multilayer optic, Osmic Confocal Max-Flux 2D-detector, and Mar345 Image Plate.

Density A LiquiPhysics Excellence DM40 density meter from Mettler Toledo with a measurement range of 0 to 3 g cm^{-3} and an accuracy of $1 \cdot 10^{-4}$ g cm^{-3} was used for all density measurements.

Results and discussion

I. Solution behavior in thermodynamically good solvents

The sample PG4 dissolved in a thermodynamically good solvent, namely dioxane, was characterized by SLS and DLS at room temperature. Figure 2 shows the Zimm diagram for this sample. The extrapolations $c \rightarrow 0$ and $q \rightarrow 0$ result in a weight-average molar mass of $M_W=(2.3\pm0.05)\cdot10^7$ g mol^{-1} and a radius of gyration of $R_G=128\pm3$ nm, as well as a positive value of the second osmotic virial coefficient $A_2=(2\pm0.1)\cdot10^{-9}$ mol dm^3 g^{-2}. Moreover, the same sample was dissolved at room temperature in another thermodynamically good solvent, namely chloroform, and was characterized by the same procedure (see Fig. SI-1 in Electronic Supplementary Material, ESM). Comparable values within the standard deviation of $M_W=(2.3\pm0.05)\cdot10^7$ g mol^{-1}, $R_G=135\pm3$ nm, and $A_2=(3\pm0.1)\cdot10^{-9}$ mol dm^3 g^{-2} were obtained, which implies that the characterization pertains to molecularly disperse solutions of PG4. Furthermore, a critical overlap concentration of $c^*=3\,M_W/4\pi\,N_A\,R_G{}^3=4.3$ g L^{-1} was calculated. Thus, all further experiments were performed using dilute solutions with polymer concentration $c<c^*$ to avoid effects of intermolecular polymer–polymer interactions.

The numerical value of $L_c=1060$ nm was determined by SLS corresponding to M_W (*vide supra*), $M_{mon}=5{,}428$ g mol^{-1} and assuming a repeat distance per monomer of $d=0.25$ nm in accordance with previous work [29]. Furthermore, from these SLS results, the persistence length l_p of the wormlike molecules are obtained from the $c/R(q)$ vs q^2 plot [39, 41] in the linear regime depending on temperature T. For PG4 in dioxane, a value of $l_p=7.0$ nm at $T=25$ °C and $l_p=8.0$ nm at $T=40$ °C is determined (see Fig. S-2 in ESM). It should be noted that here a weak influence of a minor fraction of aggregated molecules (seen at low q values) is neglected, which is not the case for the Zimm diagram shown in Fig. 2. A more refined analysis of the light scattering data based on the approach first described by Benoit and Doty [41] gives values for l_p approximately double as large under the assumption that the polydispersity index is PDI=2. However the polydispersity is not exactly known for the present sample, but in previous studies, values of PDI ≈ 2 were published for the same type of polymer [31]. It should be mentioned that the effect of the polydispersity on the estimation of molecular

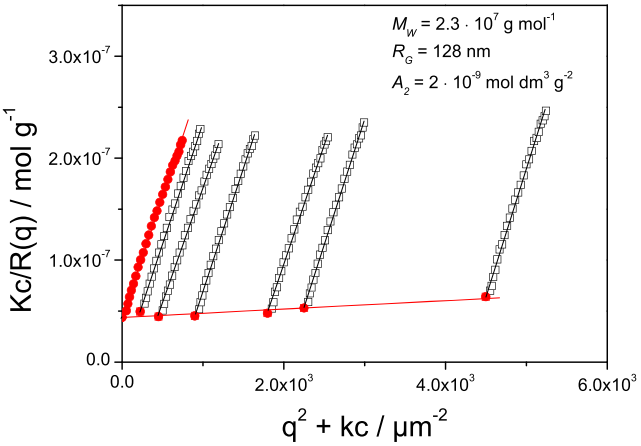

Fig. 2 Zimm diagram of sample PG4 in dioxane at $T=25$ °C

parameters such as L_c and l_p is moderate and further detailed investigation under the consideration of correction functions for polydispersity effects in wormlike chains is beyond the scope of the present work. In the further text, we take the persistence length obtained from a plot of $c/R(q)$ vs q^2 as the lower bound of l_p.

Dynamic light scattering experiments probe the micro-Browian motion which is the thermally activated free diffusion of dissolved macromolecules, in other words, DLS probes the hydrodynamic behavior of solved single molecules. It is common to express the results in terms of a field correlation function (see "Experimental section") [36]. Figure 3 shows the single mode relaxation function $C(q, t)$ of sample PG4 solved in dioxane with $c=1$ g L^{-1} along with the data evaluation by using a stretched exponential (KWW) function (see "Experimental section" for details). The distribution of relaxation times τ is described by a shape parameter of $\beta=0.85$. Fitting of the experimental data $C(q, t)$ by a KWW function is plausible in the light of further data which indicate that the DPs are to be described as soft filaments that undergo thermally induced shape fluctuations as well as micro-Brownian motions. The translational diffusion coefficient $D_0=2.5\cdot10^{-8}$ cm^2 s^{-1} obtained from the intercept of the linear variation of the q-dependent relaxation rate Γ/q^2 vs q^2, as presented in the inset of Fig. 3, enabled the calculation of a z-average Stokes–Einstein hydrodynamic radius of $R_h=72\pm2$ nm. A data evaluation by using the CONTIN method results a value of $R_{h\,CONTIN}=74\pm2$ nm, which is in very fair accordance (see Fig. S-3 in ESM).

Density and topology Foregoing work [31] has demonstrated that DPs can be described as wormlike structures. The volume of the wormlike chain (Porod–Kratky) [42] of PG4 is defined by $V_w=\pi\ R_c{}^2\ L_c=26.1\cdot10^3$ nm^3 (case a), where $R_{c\,(SAXS)}=2.8$ nm is the cross-section radius as indicated exemplary in Fig. 1 and obtained by SAXS measurements of the dry material (see Fig. 4). Taking the value of the cross-section

radius of PG4 determined by MD simulations [22, 43] $R_{c\ (MD)}$=4.0 nm as the maximum radial extension of the corona segments, i.e., where the radial segment density approaches zero, a value of V_w=53.2·10^3 nm^3 (case b) is obtained. The latter value would also be consistent with data obtained for solutions in methanol by small angle neutron scattering (SANS) experiments (unpublished results of Sigel RL, Schurtenberger P (2011) University of Fribourg, Switzerland) and therefore reflects the maximum extension of the corona segments swollen to maximal extension with methanol (for SANS). The volume occupied by the wormlike chain in its random flight conformation in the solvent dioxane at room temperature is given by V_c=4/3 π R_G^3=8.8·10^6 nm^3. Therefore, the volume filling by the wormlike chain can be approximated by 100·V_w/V_c that is 0.3 % for case a and 0.6 % for case b. Thus, the degree of volume filling is a factor of at least 10^3 larger than typically observed for classical polymers like PMMA or poly(styrene). This indicates that excluded volume effects must play a considerably large role in the definition of the persistence length l_p when comparing samples of largely different L_c. Since we investigate the solution behavior of a single polymer sample, we will not attempt to separate excluded volume effects from other effects which control the overall chain conformation. Nevertheless, it is relevant to point out that generalization of the results of our work to all chain lengths needs a detailed consideration of excluded volume effects and its consequences for the random dimension of the macromolecules. For example when establishing the calibration for size exclusion chromatography, this needs to be carefully considered otherwise erroneous conclusions will result.

At this point, a short discussion of the density ρ of the polymer may be of interest. We like to restrict the discussion

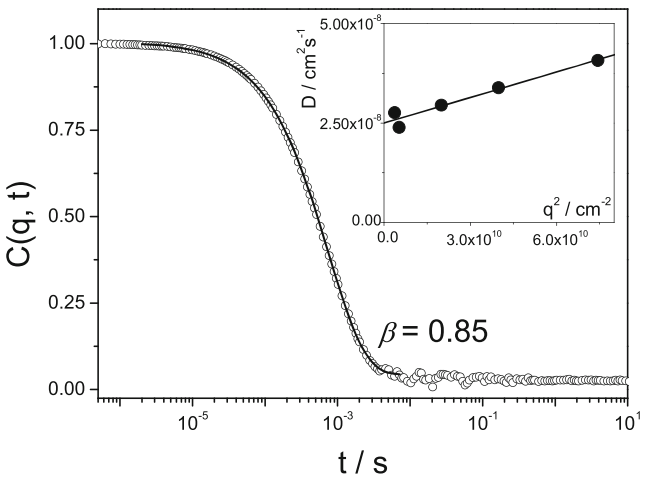

Fig. 3 Normalized field correlation function $C(q, t)$ of sample PG4 in dioxane with c=1 g L^{-1} at a scattering wave vector q=1.997·10^{-2} nm^{-1} (*open symbols*) at T=25 °C along with the corresponding KWW fit (*solid line*) characterized by a shape parameter β=0.85. The diffusion coefficient D_0 is obtained from the intercept of the linear variation of $D=\Gamma/q^2$ as a function of q^2, as shown in the *inset*

to the sample PG4 where data obtained by different techniques are available (*vide infra*). There is general agreement that spherical dendrimers and dendronized linear polymers exhibit a dense packing of the dendron segments in the interior and that the density decreases at the periphery in the manner of an error function [43, 44]. A detailed description of the density profile based on MD simulations can be found in the most recent literature [22]. However, these simulations lack experimental verification so far.

The value R_1 defines the radius at which the density of the "hard" core starts to deviate toward the lower density of the dendron segments at the periphery of the corona. This could be probably the radius relevant to describe the bending stiffness of the wormlike molecule (*vide infra*). R_2 describes the average radius of the wormlike chain in solution and/or in the solid state where the chain–chain interaction is dominated by the equilibrium between attractive and repulsive forces between different chains and/or segments of the same chain in a random flight conformation. Finally R_3 relates to the radius of maximal extension of structural elements of the corona at which density differences between solvent and polymer attached dendrons vanish. R_3 is relevant to scattering experiments, e.g., SAXS or SANS. The radius relevant to describe the self-avoiding walk in the random coil conformation would probably be located between R_2 and R_3. If one follows the results of MD simulation [22, 43], the difference $\Delta R=R_3-R_1$ is of the order of 1.4 nm and R_2=3.3 nm for PG4. The density of the hard core volume was found to be ρ=1.18 g cm^{-3} in these simulations, based on a "united atom" type of approach and did not consider solvent incorporation. As shown later, this value is close to that which we have determined for the density of this polymer dissolved in chloroform.

Furthermore, SAXS reveals for bulk (PG4 obtained by freeze-drying solutions in dioxane) the observation of Bragg peaks typical for hexagonally dense packed cylindrical objects (see Fig. 4) that allows the set-up of a unit cell in which the center-to-center distance between next neighbor cylinders is a=5.5 nm and therefore $R_{c\ (SAXS)}$=2.8 nm. In addition, the density of the material in a unit cell is given by $\rho_x=M_{mon}/V_{el}$ N_A=1.43 g cm^{-3} with V_{el} the volume of the elementary cell. Eventually, one may also consider the density of a cylinder with square box dependence of ρ for $R_{c\ (SAXS)}$=2.8 nm which gives $\rho'_x=M_{mon}/\pi\ R_c^2\ d\ N_A$=1.46 g cm^{-3}. One may associate ρ_x with the density of a cylinder with effective radius R_2 in the dry state. The density of PG4 in solution is accessible measuring the density of solutions at known weight fraction w_2 of solute. With the approximation that the measured density of the mixture $\rho_m=w_2(\rho_2-\rho_1)$, where the subscripts 1 and 2 refer to the solvent and solute, respectively, and $w_1+w_2=1$, the density of the DP ρ_2 in the dissolved state can be estimated for dioxane at room temperature. A value of ρ=1.21±0.03 g cm^{-3} for dioxane and ρ=1.11±0.03 g cm^{-3} for chloroform is calculated. In other

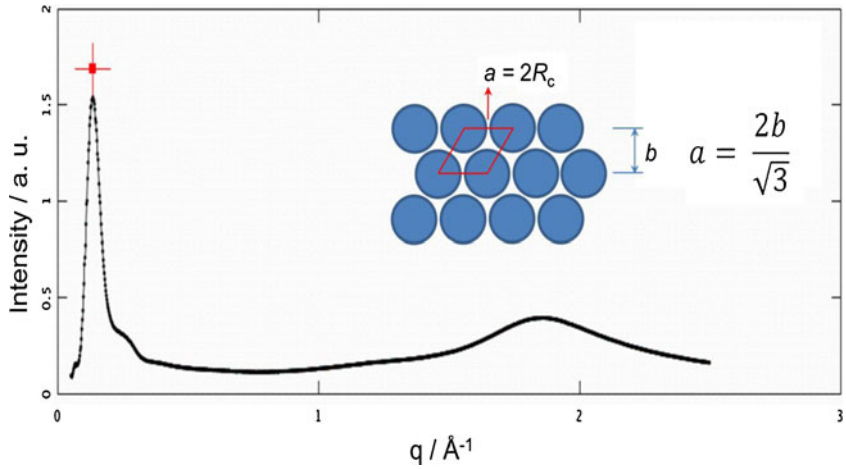

Fig. 4 Experimental SAXS curve measured at a dry sample of PG4

words, the DPs undergo substantial swelling by dissolution. The bond connectivity along the chain trajectory enforces that the swelling is two-dimensional in nature that is stretching of the dendron segments occurs in radial direction. The density ρ_x refers to the density of the bulk material in the form of hexagonally close packed cylinders and contains the contribution of the interstitial volume. However, ρ'_x refers to the density of individual cylindrical objects void of any solvent ("dry" state). Therefore ρ'_x is the proper reference to assess the degree of swelling of the object equilibrated with solvent. The degree of swelling is given by $Q=100\ (\rho'_x/\rho_{solvent})=\sim 120$ % for dioxane and ~130 % for chloroform accordingly. The swelling induces a growth of R_c from 2.8 to 3.1 nm in dioxane and 3.2 nm in chloroform.

The radial extension of PG4 dissolved in methanol was determined by SANS (unpublished results of Sigel RL, Schurtenberger P (2011) University of Fribourg, Switzerland). Two limiting data sets are available. On one hand, a value of $R_{c\ (SANS)}=2.6$ nm has been determined for PG4, which corresponds to our definition of the hard core radius. On the other hand, a second value $R_{c\ (SANS)}=4.0$ nm was obtained by a more refined analysis of the SANS data (unpublished results of Sigel RL, Schurtenberger P (2011) University of Fribourg, Switzerland) and this value refers to the maximum extension of the methanol-swollen sample PG4. The difference $\Delta R=R_3-R_1$ corresponds to the expectations of MD simulations [22, 43]. Since Q can be considered as characteristic for the thermodynamic quality of the used solvent, we conclude dioxane < chloroform < methanol for the respective solvent quality.

We note that previous work [45] of some of the authors has extensively elaborated what the proper value of the density of the same polymer, namely PG4, might be. The present findings corroborate the assumptions made in the context of interpretation of molecularly resolved images of individual chains that had been weakly absorbed to the surface of mica, highly oriented pyrolytic graphite or amorphous carbon. Zhang et al. [45] give an estimate value of $1.35\leq\rho\leq1.45$ g cm^{-3} for the dry sample and $\rho=1.1$ g cm^{-3} for the same polymer in solution. Thus, these data are in fair agreement with the present results and also correspond qualitatively with available MD simulations [22].

The swelling of the corona originates from both enthalpic and entropic effects. The main contribution to the latter is the osmotic pressure of the solvent which acts as a diluent for the segments of the dendrons. However, there are also effects due to the heat of mixing to be expected and one will generally formulate $\Delta g_{mix}=\Delta h_{mix}-T\Delta s_{mix}$ where Δg_{mix} is the free energy change per dendron of generation G upon dissolution, Δh_{mix} is the respective enthalpy change (heat of mixing), and Δs_{mix} is the entropy change. The entropy of mixing has been extensively considered in the recent literature [20, 21]. The consequences in terms of chain stretching that are increase in persistence length in thermodynamically good solvents have been pointed out to the extent that scaling laws have been formulated. These scaling laws do not predict the magnitude of the present experimental findings but merely describe the observed trends. For instance, experimentally one finds substantially different values for l_p for different solvents, e.g., for sample PG4 $l_p=12$ nm in methanol and 7.0 nm in dioxane. As mentioned earlier, the magnitude of l_p given here needs to be considered as the lower bound. It should be noted, however, that measurements of the heat of mixing solvents and DPs would be most interesting and could help to understand the role of solvents in the molecular mechanics of the swollen wormlike chain much better.

While computer-based molecular dynamics simulations [22] give reasonable prediction of the density profile normal to the backbone trajectory, they will fail in the prediction of the overall topology of the DP, notably the persistence length. The reason is that the computer simulation considers local relaxation processes of the dendron branches on the time scale $10^{-12}\leq t\leq10^{-9}$ s while the global structure of the whole chain is the result of the viscoelastic response of the DP to the thermal fluctuations in the solvent bath in which the polymer is observed by, e.g., DLS, that is the time window of $10^{-7}\leq t\leq10^{3}$ s.

II. Solution behavior in a thermodynamically poor solvent

In the course of the investigation of the solution properties of PG4 in different solvents, it was revealed that toluene acts as a thermodynamically poor solvent and may be considered as a theta-solvent (θ solvent). A freshly prepared sample of PG4 could be completely dissolved at $T>30$ °C and turbidometric investigations at various concentrations indicated that the θ temperature T_θ was slightly below 30 °C (not shown). This prompted a detailed study of dilute solutions of PG4 in toluene by SLS and DLS experiments. From the static light scattering intensity, R_G and l_p were obtained as described before (see Fig. SI-4 in ESM). Furthermore, DLS gave the time correlation function $C(q, t)$ which was interpreted in terms of a KWW distribution of the diffusion times (see "Experimental section" and Fig. 7). The further discussion will demonstrate that data analysis in terms of a KWW fit captures the physical reality in an appropriable manner, while the conventional data treatment via CONTIN [46] delivers a physically less realistic impression of individual diffusion processes contributing to the overall $C(q, t)$. The pertinent data obtained by SLS and DLS are summarized in form of a graph in Fig. 5.

Regime I and molecular mechanics of the wormlike chain As shown in Fig. 5, both R_G and R_h reveal a strong T dependence. In the following, the data are discussed according to three temperature regimes (as indicated in Fig. 5) which refer to quite different situations: Regime I refers to homogeneous solutions of molecularly dispersed chains of PG4 at $T>T_\theta$. The θ temperature is identified in the context of this work as the temperature where R_G is maximal. Within the small regime II, which extends between $24\leq T\leq 28$ °C, both SLS and DLS (see Fig. 5) gave evidence of the presence of individual molecules over extended periods of time, namely hours to days, while in regime III at $T<24$ °C strong turbidity and sedimentation appear as a sign of coagulation and the formation of large aggregates.

Since one can take R_G^2 as the characteristic magnitude to describe the dimension of a polymer in solution, the ratio of $R_G(T)^2$ over $R_G(T_\theta)^2$ gives a vivid description of the changes in the chain dimension above and below T_θ. A very strong decrease in the dimension of the individual macromolecules both, above and below T_θ, is observed, albeit for very different reasons.

The high temperature regime I First we investigate the high-temperature regime I ($T>T_\theta$). Here, we follow the argument of Flory [18, 47] and extract the temperature coefficient

$$C=\frac{\partial \ln\left(R_G^2\right)}{\partial T} \qquad (2)$$

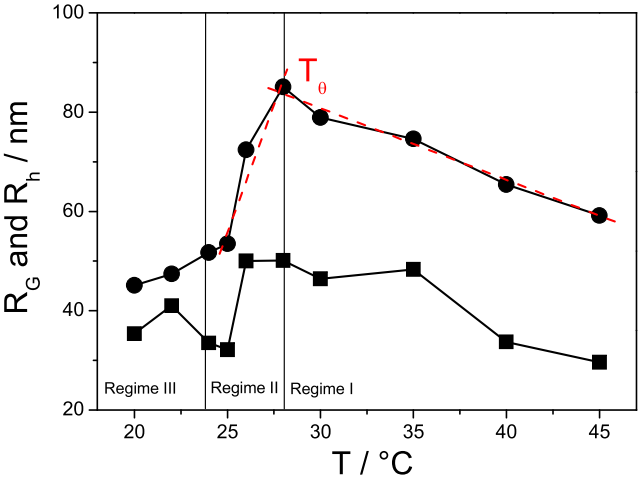

Fig. 5 Temperature dependence of radius of gyration R_G (*black circles*) and hydrodynamic radius R_h (*black squares*) of PG4 solved in toluene at a concentration of $c=1$ g L^{-1}. The *dashed red lines* denote the identification of T_θ as the maximum of R_G. The *solid lines through the data points* serve merely as a guide to the eyes

From the graph shown in Fig. 6, we derive a value of $C=-3.8\cdot10^{-2}$ K^{-1} that is a very strongly negative coefficient. Remembering a value of $C=-0.37\cdot10^{-3}$ K^{-1} for poly(styrene), 0.09 K$^{-1}<C<0.28\cdot10^{-3}$ K^{-1} for poly(isobutylene), and $C=-0.23\cdot10^{-3}$ K^{-1} for poly(oxyethylene) [18, 47], the most unusual behavior of PG4 comes to the surface. The latter shows a 100-fold stronger temperature dependence of the coil dimension on T in toluene as compared to conventional linear macromolecules. The reason for this surprising behavior becomes obvious looking to the changes in l_p with T obtained from analysis of the SLS data (see ESM). The persistence length decreases from a value of $l_p=7.0$ nm at $T=T_\theta=28$ °C to 5.8 nm at $T=45$ °C, the highest temperature for which data are available. The data indicate an approximately linear decrease of l_p with T in this limited temperature range with a slope of $dl_p/dT=-0.07$ nm K^{-1}. These results can also be described in the picture of a wormlike chain in which the number of statistical elements which describe the random flight trajectory of the object changes with T (unlike in classical chains). Accordingly, we can calculate the number of statistical elements N per chain by $N=L_c/l_k$. N changes from a value of 295 statistical elements per chain at $T=28$ °C to 356 at $T=45$ °C, which is a change by ca. 20 % over a temperature difference of 17 K. This interpretation is corroborated by the extrapolation of the data for the T dependence of l_p in Fig. 6 to 20 °C, which neglecting the occurrence of the θ behavior at $T<T_\theta$ gives a value of ~7.5 nm which coincides very well with our experimental data found for solution in dioxane. The latter is a thermodynamically good solvent for the segments of the dendrons (*vide supra*). We conclude that the viscoelastic interactions among the branches of the dendrons that form an entanglement network (see Fig. 1) are dominating the elastic behavior of the

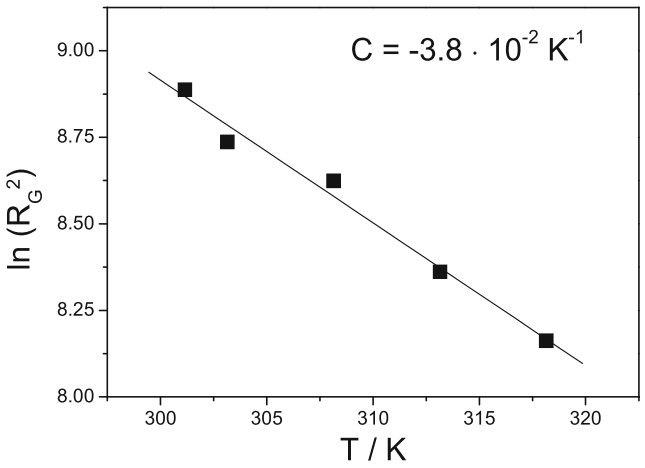

Fig. 6 Temperature dependence of the unperturbed dimension of PG4 molecules solved in toluene at $T>T_\theta$; $\partial\ln(R_G^2)/\partial T=-3.8\cdot10^{-2}$ K^{-1}

wormlike chains in the poor solvent. The solvent itself acts as a plasticizer in this case.

The connection of l_p to the molecular mechanics of the wormlike chain is straight forward. The persistence length l_p reflects the Young's modulus E of the wormlike chain according to [48]

$$l_p = C_0 \frac{E}{k_B T} \tag{3}$$

where the Boltzmann k_B is constant and where the coefficient C_0 according to Odjik [48] refers to the topology of the cylindrical object by $C_0=(\pi/64)D^4$ with $D=2R_c$ being the diameter of its cross section. In other words, the T dependence of l_p and thereby R_G is interpreted as a strong T dependence of the modulus of the chain since there is no reason to assume changes in the topological term, namely D^4 in this temperature regime.

To bring out the temperature dependence of the modulus more clearly, a plot of $l_p\cdot T$ vs T is shown in Fig. 7. The slope indicates a 0.75 (~1)% linear decrease in modulus per degree in the small temperature range investigated here and under the assumption that C_0=constant. Moreover, these data give evidence that fluctuations in the modulus along the chain trajectory must occur since the energy required for bending is only a few k_BT.

In other words, micro-Brownian motion of the macromolecules and bending fluctuations fall into the same spectral window to be seen by light scattering experiments and this situation is reflected by the KWW distribution of relaxation times seen in the DLS spectra (see Figs. 3 and 8). These results also shed light onto the nature of the corona around the polymer backbone which is composed of the dendrons. We like to describe the material in the bulk of the corona as a gel with strongly T-dependent shear modulus. Therefore, what is observed as T dependence of R_G and of l_p is a reflection of the molecular dynamics of the solvent swollen DPs close to the glass transition temperature T_g. The dry sample PG4 showed T_g=~70 °C [20, 35]. However, the precise value needs further discussion since the T_g region is unusually broad. Treating the role of the solvent as that of a plasticizer, one can interpret the data in terms of the viscoelastic behavior of a gel cylinder of given molecular dimensions. Close and around T_θ, the modulus of all polymers show a strong T dependence.

The formula of Odijk [48] describes the mechanics of a cylindrical rod of homogeneous elasticity and homogeneous density. This is, of course, an idealization as already pointed out by Odijk himself but helps to define an equivalent object which shows the observed behavior of the real molecule. Moreover, Eq. 3 gives the scaling with diameter at given elastic constant.

For instance, plugging the value of l_p=7.2 nm found for PG4 in dioxane at T=25 °C (*vide supra*) into Eq. 3 and assuming that $E/k_BT=1$ gives R_c=1.74 nm which is in very reasonable agreement with the experimental result discussed above having in mind that the real molecule exhibits a radial dependence of ρ and thereby of the modulus as well. Assuming a value $E/k_BT=2$ would decrease the magnitude of R_c to 1.46 nm, that is further away from the experimentally observed value of R_c. For methanol as solvent, a value of l_p=12 nm has been reported (unpublished results of Sigel RL, Schurtenberger P (2011) University of Fribourg, Switzerland). Again, setting $E/k_BT=1$ gives R_c=1.98 nm in reasonable agreement to what has been observed by SANS measurements ($R_{c\ (SANS)}$=2.6 nm).

The findings suggest that the diameter of the equivalent cylinder with a stiffness as defined by Eq. 3 is approximately 75 % of the radius estimated from SANS or density measurements in solution. This conclusion holds for PG4 and under the further assumption that $E/k_BT=1$. Moreover, E is obviously different for different good solvents as reflected by the

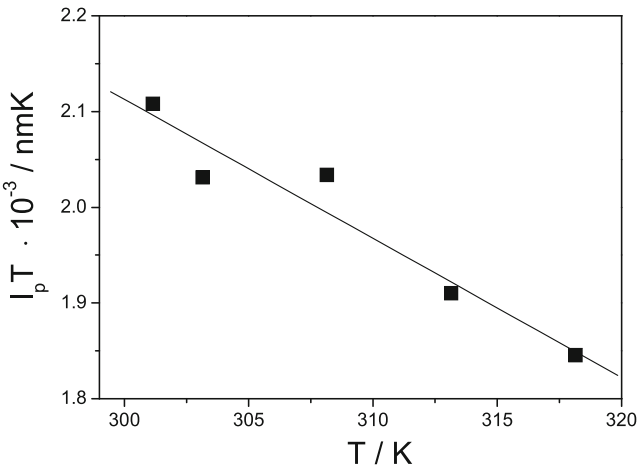

Fig. 7 Temperature dependence of the Young's modulus E for PG4 dissolved in toluene at a concentration of c=1 g L^{-1} in a temperature range of 28 °C≤T≤45 °C

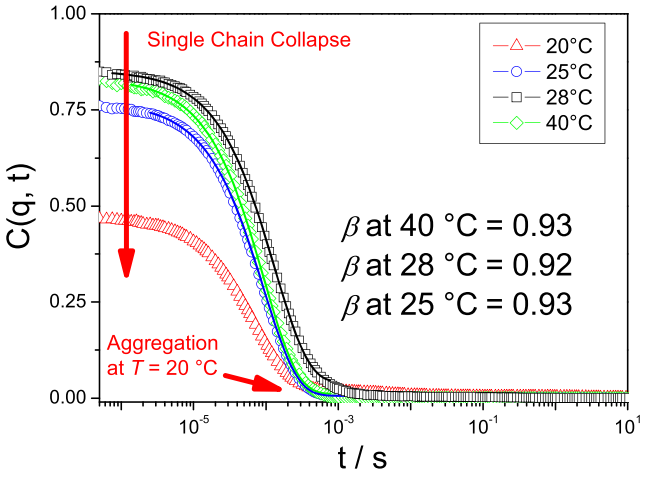

Fig. 8 Normalized field correlation functions $C(q, t)$ of sample PG4 in toluene at c=1 g L^{-1} at a scattering wave vector q=1.997·10^{-2} nm^{-1} at different temperatures T (*open symbols*) along with the corresponding KWW fit (*solid lines*), the shape parameter β characterizes the distribution of relaxation times

dependence of l_p on solvent quality. Furthermore, we cannot assume that E is independent on G. As the number of generations of DPs becomes smaller, the molecular object is less well described by a square box radial distribution of density and modulus. In other words, the boundary conditions which are neglected in Eq. 3 become more and more relevant in a manner which would best be covered by simulations and not by analytical formulations as the one given by Odijk [48]. Of course, one can always define an equivalent object which would behave as the molecule under investigations, meaning that l_p can be correlated to virtual cross sections at given values of E/k_BT. However, the interpretation of the meaning of D and its correlation with chemical structure elements will be a task of further work. So far, we have followed the formulation given by Odijk [48] for the case of a stress-free wormlike chain which is in equilibrium with a thermal bath, i.e., dissolved in a θ solvent. It is worth mentioning that Odijk [48] has considered the case of identical chains under stress as well, that is the eigen-modes of a filament under tension leading to periodic undulation of the chains. The wavelength of the undulation depends on the applied tension and the temperature of the bath in which the chains are embedded. The result is of importance to the measurable end-to-end-distance of the extended wormlike chains which is not an independent parameter but depends on the quality of the thermal excitations of the filaments. This aspect has been subject of a number of theoretical and experimental investigations in the context of developing the biomechanics of naturally occurring polymers, e.g., DNA and collagen [49–51].

While most of the work summarized and analyzed in these references point toward the mechanics of biological macromolecules and biogenic filaments as found in animal tissue, the arguments are helpful in the design of synthetic macromolecules as well. These are available in the form of brush-like and dendronized polymers. In fact, phenomena predicted by theory in the above-mentioned literature have been identified experimentally for polymer brushes by Gunari et al. [52]. The predicted thermally activated undulation effects were revealed measuring force–extension curves on individual macromolecules. Analysis of their data in the light of the above mentioned studies allowed them to determine precise values of l_p for the brush-like polymers. We like to note that the interesting case of filaments composed of mechanically heterogeneous elements has also been treated in terms of a theoretical analysis [53]. Translated into the language of dendronized linear polymers, this would mean a copolymer where the co-monomers differ in the chemical structure and/or generation number of the dendrons attached to the repeat units, cases which to our knowledge have only been realized in a few cases [54, 55].

Regimes II and III Regime II of the behavior of PG4 dissolved in toluene is characterized by a dramatic decrease in the average chain dimension over a narrow temperature range from $T=T_\theta$=28 °C to about 24 °C (see Figs. 5 and 8). However, both SLS and DLS indicate the presence of molecularly disperse macromolecules in stable solutions without signs of aggregation or sedimentation over days. R_G decreases by 43 % and R_h by 53 % (see Fig. 5). Accordingly, $\langle R_G\rangle/\langle R_h\rangle$ assumes a value of ca. 1.5 within this temperature regime, that is a value expected for randomly coiled Kuhn chains. Note that in regime I ($T>T_\theta$) we observed fully expanded wormlike chains of the investigated polymer and the determined value for $\langle R_G\rangle/\langle R_h\rangle$ is ~2, which correlate with the theoretical value for rod-like structures very well. Regime II is characterized by a dramatic decrease in the average chain dimension over a temperature range from $T=T_\theta$=28 °C to about 24 °C. Here, $\langle R_G\rangle/\langle R_h\rangle$ results in a value of ~1.5. For linear macromolecules with a further decrease of T ($T<T_\theta$), a very sharp coil-to-globule transition would be expected. In such a case, $\langle R_G\rangle/\langle R_h\rangle$ would be around 0.77. In the present case, the situation for dendronized polymers is somewhat different in so far that we observed a transition range between 28 and 24 °C. Within this range, meta-stable structures are observed (*vide infra*).

Going to T<24 °C, the solutions become unstable and within a short time turbidity develops rapidly accompanied by sedimentation of the formed aggregates, in other words, regime III refers to a two-phase situation of a polymer–solvent phase diagram, while in regime II, we observe a fractional desolvation of the dendron corona of PG4. This is more precisely documented by the DLS results shown in Fig. 8. In particular, the dramatic change in $C(q, t)$ is documented going from 25 °C where we still determine fluctuating individual macromolecules to 20 °C where the solution becomes unstable

(aggregation). Note the reduction of the amplitude of $C(q, t)$ at $T<24$ °C and the appearance of aggregates. The decrease in the chain dimensions with decreasing T without precipitation between 28 and 24 °C and keeping β=const.=0.9 suggests a meta-stable pearl necklace structure of partially desolvated chains. Structures of locally collapsed chain segments and still solvated stretches of segments have been identified as unstable intermediates in the kinetics of the much studied coil-to-globule transition of linear macromolecules [56, 57]. It occurs close to the θ temperature. In fact, many stages of the transition have been identified by simulation and some of them have been verified by time-resolved studies of the precipitation process as kinetic intermediates preceding the final precipitation in the form of multi-molecular aggregates. In the present case, the situation is substantially different in so far as we hypothesize that the gel-like bulk of the corona of the dendrons at first undergoes a desolvation process which leads to fluctuations of the osmotic pressure along the chain trajectory. Presumably this creates regions of fully solvated dendrons in equilibrium with regions that are fully or partially desolvated as indicated in the schematic Fig. 9. This will change the character of the wormlike chain to that of a segmented chain with strongly solvent (and temperature)-dependent segment length. This also means a fluctuating shear modulus along the trajectory of the chain. At this point, it must be left to further studies to find out what the precise segment length distribution looks like.

The foregoing description is also supported by the experimental observation that the transition around T_θ=28 °C can be completely suppressed adding 10 vol% of dioxane to the toluene solution (see Fig. SI-5 in ESM). Dioxane acts as a preferential solvent to the segments of the dendrons and the gel-like character of the corona remains intact even if the toluene becomes a non-solvent at $T=T_\theta$.

Figure 9 describes schematically the situation for the solution of PG4 in pure toluene in terms of a phase diagram. A homogenous solution of wormlike chains corresponding to regime I exists above T_θ, where the dendron corona is homogeneously swollen by the solvent toluene. At T_θ, the intramolecular segregation of dendron segments and solvent starts leading to a locally fluctuating solvent concentration along the trajectory of the macromolecules. Macroscopic phase separation will only occur below 24 °C when the length of the dissolvated regions per macromolecule exceeds a critical value. The process of desolvation is depicted in Fig. 10 and is assumed to occur inside the shaded regime of the phase diagram shown in Fig. 9.

The description given by Fig. 10 bears similarity to what has been extensively discussed for the occurrence of Rayleigh instabilities in thin jets of liquids as well as transition of rod-like filaments or particles to spheres in the solid state [58, 59]. In fact, given the topology and dimensions of DPs, one would expect that Rayleigh instabilities must occur

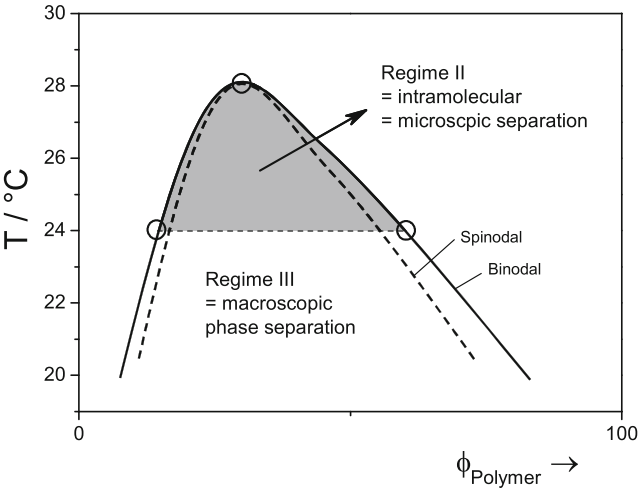

Fig. 9 Schematic phase diagram in terms of temperature T vs volume fraction φ for PG4 dissolved in toluene at a temperature range of $T \leq T_\theta \leq 28$ °C

but need to remain incomplete because of the bond connectivity of the polymer main chain. Furthermore, we cannot associate a surface tension vs bulk energy competition as the driving force for the perturbation of the shape. Rather, we invoke a competition between enthalpic and entropic forces acting on the solvent embedded macromolecule. The entropic forces are mainly to be associated to the osmotic pressure of the solvent which likes to swell the bulk of the DPs to the maximum extent while the enthalpic forces refer to the heat of mixing of solvent and branches of the dendrons. The θ temperature would then be understood as $T_\theta=\Delta H_{mix}/\Delta S_{mix}$. This treatment is common in all theories of the phenomena of the swelling of polymer gels [27]. Below T_θ fluctuations of solvent concentration inside the bulk of the corona of the DP occur, which can also be described as fluctuations of the cross section. This is shown in Fig. 10. The minimum cross-section diameter for PG4 is obviously the one of the dry polymer ($2R_{c\ (SAXS)}$=5.6 nm, *vide supra*) and the maximum diameter must be in the order of 6 nm for the solvent swollen PG4. Following the literature and without further proof, we assume that the fastest growing wavelength of the shape fluctuation dominates the topology by

$$\lambda = 2\sqrt{2R_{max}} \tag{4}$$

with R_{max}=3 nm, this yield 6 nm as the order of magnitude for λ which is not surprisingly of the same magnitude as the persistence length observed for this situation in the regime II for PG4.

One needs to emphasize that Fig. 10 depicts merely the local structure of the polymer in toluene at T=24−28 °C but not the global structure. At present, we have little information on the global structure except values for R_G and R_h (see Fig. 5). However, the foregoing discussion sheds light onto the mechanism of chain collapse below T_θ. The DPs can be

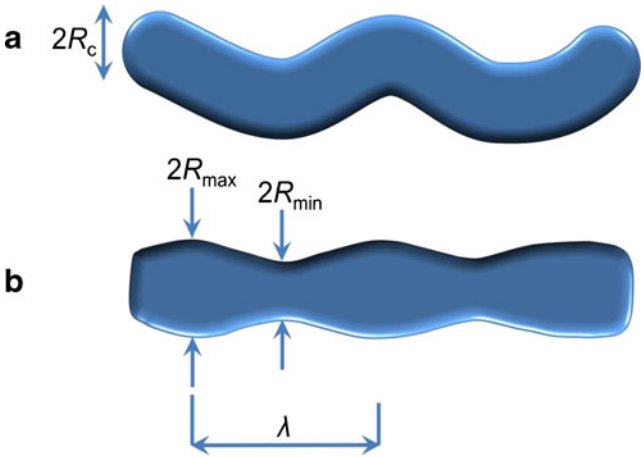

Fig. 10 Schematic illustration of the θ solvent induced local changes of the basically cylindrical topology of DPs. A decreasing temperature T results in a transformation from wormlike chains at $T>T_\theta$ (**a**) to pearl necklace structures below the θ temperature T_θ (**b**). λ represents most probable wavelength of the shape perturbation. The pearl necklace structure presumably exists in the shaded regime of the phase diagram shown in Fig. 9

seen as anisotropic colloidal objects. In good solvents, the formation of aggregates is prevented by an osmotic barrier which acts against interpenetration of the surface dendron branches of different parts of the same as well as different wormlike chains. In other words, and following DLVO theory [24–26] and later modifications for steric stabilization of colloids among them most notably latex suspensions [28], the individual DP is subject to osmotic stabilization in good solvents. A schematic diagram that displays the interaction potential W between two segments of the DPs vs their distance H is shown in Fig. SI-6 in ESM. The interaction energy is repulsive for thermodynamically good solvents (W_S) at distances $H \leq 2R_c$ neglecting terms which describe hydrodynamic interactions. However, attractive forces create a minimum in the energy curve for thermodynamically poor solvents (W_θ). For a θ solvent, we assume that the magnitude of the attractive force ΔW between two segments can be approximated by $k_B T_\theta$. In consequence at $T>T_\theta$, the thermal energy is sufficient to screen the attractive interactions.

In poor and θ solvents, the osmotic stabilization fails and contacts between different parts of the same chain and/or different chains are now favored because local interpenetration of the branches of the dendrons relieve packing stress. Dendron branches of one chain replace solvent molecules in another chain. This results in an overall attractive force and stabilizes chain–chain contacts.

Returning to the case presented here, for PG4, we can now interpret the observation of a temperature regime below T_θ in which still individual chains exist in solution. The still solvated parts of the wormlike chain offer sufficient osmotic stabilization to hold the individual colloidal objects in solution. This situation may be further stabilized by a redistribution of the still solvated regions towards the outside of the volume occupied by the chain in its random walk conformation, in other words by a partial collapse of the whole structure into regions of higher and lesser solvation of the dendrons.

While these considerations are of course rather hypothetical, they may nevertheless serve as a valuable platform or working hypothesis for further investigations.

Conclusions

This work presents data on the structure of dendronized linear polymers in solution. Both cases of solutions in thermodynamically good and poor solvents (θ solvent) are considered. Although the data are only presented for a single sample, a DP of fourth generation and contour length of 1,060 nm ($M_W=2.3\cdot10^7$ g mol^{-1}), it is suggested that the results can be generalized and point out how and why DPs differ principally from conventional polymers.

The branches of the dendrons form an entanglement network which undergoes swelling in the solvent in which the polymer is dissolved. Substantial swelling of the cross-section radius is experimentally observed. The osmotic pressure of the solvent stretches the chain trajectory as indicated by the solvent-dependent persistence length in thermodynamically good solvents. In poor solvents, the solvent itself can be considered as a plasticizer of the entanglement network of the branches of the dendrons at temperatures above the θ temperature. Following Odijk's [48] argumentation, the persistence length can be interpreted as the product of a topological term related to the cylindrical geometry of the DPs and a term which pertains the interplay between Young's modulus of the macromolecule and the thermal force acting on the object in solution (E/k_BT). In other words, the DP is seen as a filament of a cross section that depends on the chemical structure of the dendrons and the degree of swelling in the respective solvent at given temperature. The shape persistence is, therefore, of a different nature than in conventional polymers where either steric hindrance or bond configurations produce solvent-independent chain extension [60]. In good solvents, the osmotic pressure takes care of maximum swelling and this counteracts thermal fluctuations of the chain trajectory. In poor solvents, the viscoelastic nature of the entanglement network of the branches of the dendrons comes into play. The consequence is a strongly temperature-dependent modulus of the filament resulting in a strong and unusually large temperature dependence of the radius of gyration. Moreover, the incompatibly of solvent and dendron segments induces local shape corrugations at a temperature defined by $T_\theta=\Delta H_{mix}/\Delta S_{mix}$ where ΔH_{mix} and ΔS_{mix} refer to the heat of mixing of the dendrons and the respective entropy of mixing. This is seen as the driving force for the

precipitation, that is phase separation of solvent and polymer as a critical wavelength of the fluctuations is surpassed.

In summary, the DP is regarded as a colloidal object in which the attractive and repulsive forces between different parts (segments) of the same chain and/or between different chains are dominated by forces commonly described in the frame of the DLVO theory. In particular, the repulsive forces between different chains and/or stretches of the same chain within the same filament which hold the macromolecules in solution are to be described as osmotic barrier against interpenetration of the surfaces of the solvent swollen outer regions of the dendron corona. This is the case of steric stabilization of colloidal objects.

As the solvent is ejected from the dendron shell as consequence of temperature-dependent incompatibility, this mechanism of stabilization fails and precipitation occurs. This suggests a rather different interpretation of the processes and mechanisms behind the phenomena described by polymer phase diagrams. In other words, the conventional description in the terms of X parameters according to the Flory–Huggins theory is not appropriate for DPs. The descriptions of the DPs in terms of colloidal filaments undergoing swelling and thermal fluctuations of local and global nature deserves not only further tests but gives hints as well for potential applications. For instance, networks composed of slightly cross-linked DPs should exhibit extraordinary temperature dependence of the elastic modulus if swelled with thermodynamically poor solvent. The individual chains or filaments should exhibit properties similar to gel cylinders which have been described for their earthworm-like behavior [61, 62] in confined dimensions that is capillaries of cross section smaller than the radius of gyration which would induce stretching of the chains. Alternatively, earthworm-like behavior should be observed for chains on surfaces. In particular, mobility on rough surfaces with the structure of a ratchet should be of interest. Another major topic would be the mixing of DPs with nanoscale-sized pigments. It is expected that depletion phenomena, that is formation of clusters of particles from an initially homogeneous distribution of particles in the solvent swollen matrix of the polymer, will not occur for particles which are smaller than the characteristic dimension of the DPs that is cross-section radius and persistence length [63, 64].

Acknowledgments G. W. and A. K. are grateful to Prof. K. Landfester (Max Planck Institute for Polymer Research, Mainz) for her support of this project. The authors thank Prof. P. Schurtenberger (Department of Physical Chemistry, Lund University, Lund) and Dr. R. Sigel (Adolphe Merkle Institute, University Fribourg, Fribourg) for permission to use their SANS data. Prof. B. Chu (Department of Chemistry, State University of New York, Stony Brook) and Prof. M. Schmidt (Institute for Physical Chemistry, University of Mainz, Mainz) are gratefully acknowledged for helpful discussion and suggesting additional light scattering experiments and data evaluation procedure. We thank Dr. M. Mezger (Max Planck Institute for Polymer Research, Mainz) for the SAXS measurement and S. Seywald (Max Planck Institute for Polymer Research, Mainz) for density measurements. Furthermore, helpful discussions with Prof. G. Fytas (Department of Materials Science and Technology, University of Crete and F.O.R.T.H., Heraklion), Prof. U. Suter (Institute of Polymers, ETH Zurich, Zurich), and Prof. D. Y. Yoon (Department of Chemical Engineering, Stanford University, Stanford) are gratefully acknowledged.

References

1. Frey H (1998) From random coil to extended nanocylinder: dendrimer fragments shape polymer chains. Angew Chem Int Ed 37(16):2193–2197
2. Schlüter A (1998) Dendrimers with polymeric core: towards nanocylinders. Top Curr Chem 197:165–191
3. Schlüter AD, Rabe JP (2000) Dendronized polymers: synthesis, characterization, assembly at interfaces, and manipulation. Angew Chem Int Ed 39(5):864–883
4. Ishizu K, Tsubaki K, Mori A, Uchida S (2003) Architecture of nanostructured polymers. Prog Polym Sci 28(1):27–54
5. Zhang A, Shu L, Bo Z, Schlüter AD (2003) Dendronized polymers: recent progress in synthesis. Macromol Chem Phys 204(2):328–339
6. Andreopoulou A, Carbonnier B, Kallitsis J, Pakula T (2004) Dendronized rigid-flexible macromolecular architectures: syntheses, structure, and properties in bulk. Macromolecules 37(10): 3576–3587
7. Afang Z (2005) Synthesis, characterization and applications of dendronized polymers. Prog Chem 17(1):157–171
8. Frauenrath H (2005) Dendronized polymers—building a new bridge from molecules to nanoscopic objects. Prog Polym Sci 30(3):325–384
9. Nyström AM, Furo I, Malmström E, Hult A (2005) Bulk properties of dendronized polymers with tailored end–groups emanating from the same backbone. J Polym Sci, Part A: Polym Chem 43(19): 4496–4504
10. Carlmark A, Hawker C, Hult A, Malkoch M (2008) New methodologies in the construction of dendritic materials. Chem Soc Rev 38(2):352–362
11. Zhang A, Sakamoto J, Schluter DA (2008) Polymers going rigid, thick, and laterally infinite. Chimia 62(10):776–782
12. Rosen BM, Wilson CJ, Wilson DA, Peterca M, Imam MR, Percec V (2009) Dendron-mediated self-assembly, disassembly, and self-organization of complex systems. Chem Rev 109(11):6275–6540. doi:10.1021/cr900157q
13. Chen Y, Xiong X (2010) Tailoring dendronized polymers. Chem Commun 46(28):5049–5060
14. Xiong X, Chen Y, Feng S, Wang W (2010) Dendronized copolymers functionalized with crown ethers and their reversible modification through host–guest interaction. J Polym Sci, Part A: Polym Chem 48(16):3515–3522
15. Xiong X, Chen Y (2011) Clickable dendronized copolymers for introducing structural heterogeneity. Eur Polym J 48:569–579

16. Chen Y (2012) Shaped hairy polymer nanoobjects. Macromolecules 45(6):2619–2631
17. Paez JI, Martinelli M, Brunetti V, Strumia MC (2012) Dendronization: a useful synthetic strategy to prepare multifunctional materials. Polymers 4(1):355–395
18. Flory P (1969) Statistical mechanics of chain molecules. Interscience, New York
19. Brandrup J, Immergut EH, Grulke EA, Abe A, Bloch DR (1999) Polymer handbook, vol 1999. Wiley, New York
20. Guo Y, van Beek JD, Zhang B, Colussi M, Walde P, Zhang A, Kröger M, Halperin A, Dieter Schlüter A (2009) Tuning polymer thickness: synthesis and scaling theory of homologous series of dendronized polymers. J Am Chem Soc 131(33):11841–11854
21. Borisov O, Zhulina E, Birshtein T (2012) Persistence length of dendritic molecular brushes. ACS Macro Lett 1:1166–1169
22. Bertran O, Zhang B, Schlüter AD, Halperin A, Kröger M, Alemán C (2013) Computer simulation of dendronized polymers: organization and characterization at the atomistic level. RSC Advances 3:126–140
23. Efthymiopoulos P, Vlahos C, Kosmas M (2009) Theoretical study on the size and the shape of linear dendronized polymers in good and selective solvents. Macromolecules 42(4):1362–1369
24. Derjaguin BL, Landau L (1941) Theory of the stability of strongly charged lyophobic sols and of the adhesion of strongly charged particles in solutions of electrolytes. Acta Physico Chemica URSS 14:633–662
25. Russel W, Saville D, Schowalter W (1989) Colloid dispersions. Cambridge University Press, New York
26. Verwey EJWO, Overbeek JTG (1948) Theory of the stability of lyophobic colloids. Elsevier, Amsterdam
27. Quesada-Pérez M, Maroto-Centeno JA, Forcada J, Hidalgo-Alvarez R (2011) Gel swelling theories: the classical formalism and recent approaches. Soft Matter 7(22):10536–10547
28. Tadros T (2011) Interparticle interactions in concentrated suspensions and their bulk (Rheological) properties. Advances in colloid and interface science 168(1):263–277
29. Samadi F, Wolf BA, Guo Y, Zhang A, Dieter Schluter A (2008) Branched versus linear polyelectrolytes: intrinsic viscosities of peripherically charged dendronized poly(methyl methacrylate)s and of their uncharged analogues. Macromolecules 41(21):8173–8180
30. Shu L, Göossl I, Rabe JP, Dieter Schlüter A (2003) Quantitative aspects of the dendronization of dendronized linear polystyrenes. Macromol Chem Phys 203(18):2540–2550
31. Zhang B, Wepf R, Fischer K, Schmidt M, Besse S, Lindner P, King BT, Sigel R, Schurtenberger P, Talmon Y (2011) The largest synthetic structure with molecular precision: towards a molecular object. Angew Chem Int Ed 50(3):737–740
32. Junk MJN, Li W, Schlüter AD, Wegner G, Spiess HW, Zhang A, Hinderberger D (2010) EPR spectroscopic characterization of local nanoscopic heterogeneities during the thermal collapse of thermoresponsive dendronized polymers. Angew Chem Int Ed 49(33):5683–5687
33. Junk MJN, Li W, Schlüter AD, Wegner G, Spiess HW, Zhang A, Hinderberger D (2011) EPR spectroscopy provides a molecular view on thermoresponsive dendronized polymers below the critical temperature. Macromol Chem Phys 212(12):1229–1235
34. Kurzbach D, Kattnig DR, Zhang B, Schlüter AD, Hinderberger D (2011) Assessing the solution shape and size of charged dendronized polymers using double electron–electron resonance. J Phys Chem Lett 2(13):1583–1587
35. Zhang A, Okrasa L, Pakula T, Schlüter AD (2004) Homologous series of dendronized polymethacrylates with a methyleneoxycarbonyl spacer between the backbone and dendritic side chain: synthesis, characterization, and some bulk properties. J Am Chem Soc 126(21):6658–6666
36. Brown W (1993) Dynamic light scattering: the method and some applications, vol 49. Oxford University Press, Oxford
37. Jaskiewicz K, Larsen A, Schaeffel D, Koynov K, Lieberwirth I, Fytas G, Landfester K, Kroeger A (2012) Incorporation of nanoparticles into polymersomes: size and concentration effects. ACS Nano 6:7254–7262
38. Kratochvíl P (1987) Classical light scattering from polymer solutions, vol 79. Elsevier, Amsterdam
39. Kroeger A, Belack J, Larsen A, Fytas G, Wegner G (2006) Supramolecular structures in aqueous solutions of rigid polyelectrolytes with monovalent and divalent counterions. Macromolecules 39(20):7098–7106
40. Becker A, Kohler W, Müller B (1995) A scanning Michelson interferometer for the measurement of the concentration and temperature derivative of the refractive index of liquids. Ber Bunsenges Phys Chem 99:600
41. Benoit H, Doty P (1953) Light scattering from non-Gaussian chains. J Phys Chem 57(9):958–963
42. Kratky O, Porod G (1949) Röntgenuntersuchung gelöster fadenmoleküle. Recl Trav Chim Pay-B 68(12):1106–1122
43. Pasquino R, Zhang B, Sigel R, Yu H, Ottiger M, Bertran O, Aleman C, Schlüter A, Vlassopoulos D (2012) Linear viscoelastic response of dendronized polymers. Macromolecules 45(21):8813–8823
44. Ballauff M, Likos CN (2004) Dendrimers in solution: insight from theory and simulation. Angew Chem Int Ed 43(23):2998–3020
45. Zhang B, Wepf R, Kröger M, Halperin A, Schlüter AD (2011) Height and width of adsorbed dendronized polymers: electron and atomic force microscopy of homologous series. Macromolecules 44(17):6785–6792
46. Provencher SW (1982) CONTIN: a general purpose constrained regularization program for inverting noisy linear algebraic and integral equations. Comput Phys Commun 27(3):229–242
47. Mark J, Flory P (1965) The configuration of the polyoxyethylene chain. J Am Chem Soc 87(7):1415–1423
48. Odijk T (1995) Stiff chains and filaments under tension. Macromolecules 28(20):7016–7018
49. Holzapfel GA, Ogden RW (2011) On the bending and stretching elasticity of biopolymer filaments. J Elasticity 104(1):319–342
50. Bao G (2002) Mechanics of biomolecules. J Mech Phys Solids 50(11):2237–2274
51. Emanuel M, Mohrbach H, Sayar M, Schiessel H, Kulić IM (2007) Buckling of stiff polymers: influence of thermal fluctuations. Phys Rev E 76(6):061907
52. Gunari N, Schmidt M, Janshoff A (2006) Persistence length of cylindrical brush molecules measured by atomic force microscopy. Macromolecules 39(6):2219–2224
53. Su T, Purohit PK (2010) Thermomechanics of a heterogeneous fluctuating chain. J Mech Phys Solids 58(2):164–186
54. Xiong X, Chen Y, Feng S, Wang W (2007) Codendronized polymers: wormlike molecular objects with a segmented structure. Macromolecules 40(25):9084–9093
55. Feng S, Xiong X, Zhang G, Xia N, Chen Y, Wang W (2009) Hierarchical structure in oriented fibers of a dendronized polymer. Macromolecules 42(1):281–287
56. Wang X, Wu C (1999) Light-scattering study of coil-to-globule transition of a poly (*N*-isopropylacrylamide) chain in deuterated water. Macromolecules 32(13):4299–4301
57. Wu C, Wang X (1998) Globule-to-coil transition of a single homopolymer chain in solution. Phys Rev Lett 80(18):4092–4094
58. Karim S, Toimil-Molares M, Balogh A, Ensinger W, Cornelius T, Khan E, Neumann R (2006) Morphological evolution of Au nanowires controlled by Rayleigh instability. Nanotechnology 17(24):5954
59. Nichols F (1976) On the spheroidization of rod-shaped particles of finite length. J Mater Sci 11(6):1077–1082

60. Wegner G (2003) Shape persistence as a concept in the design of macromolecular architectures. Macromol Symp 201(1):1–10
61. Arora H, Malik R, Yeghiazarian L, Cohen C, Wiesner U (2009) Earthworm inspired locomotive motion from fast swelling hybrid hydrogels. J Polym Sci, Part A: Polym Chem 47(19):5027–5033
62. Yeghiazarian L, Mahajan S, Montemagno C, Cohen C, Wiesner U (2005) Directed motion and cargo transport through propagation of polymer–gel volume phase transitions. Adv Mater 17(15):1869–1873
63. Demir MM, Castignolles P, Akbey Ü, Wegner G (2007) In-situ bulk polymerization of dilute particle/MMA dispersions. Macromolecules 40(12):4190–4198
64. Demir MM, Wegner G (2012) Challenges in the preparation of optical polymer composites with nanosized pigment particles: a review on recent efforts. Macromol Mater Eng 297(9):838–863